Antarctic Science 8 (1): 61–72 (1996)

Palaeomagnetic results from the middle Tertiary Meander Intrusives of northern Victoria Land, East Antarctica

ELENA BELLUSO[1] and ROBERTO LANZA[2]

[1]Dipartimento di Scienze Mineralogiche e Petrologiche, Università di Torino, via Valperga Caluso 35, 10125 Torino, Italy
[2]Dipartimento di Scienze della Terra, Università di Torino, via Valperga Caluso 35, 10125 Torino, Italy

Abstract: The Tertiary stocks (Meander Intrusives) cropping out along the coasts of the Ross Sea were sampled for a palaeomagnetic study during the sixth Italian expedition to northern Victoria Land. Laboratory investigations concerned magnetic mineralogy and remanent magnetization. Minerals of the magnetite-ulvöspinel series occur in the rocks from all stocks, with low-Ti titanomagnetite usually prevalent. Haematite and goethite occur in small amounts as alteration products. Large secondary components commonly screen the characteristic remanent magnetization and were removed by thermal or AF demagnetization at temperatures or peak-fields higher than 360°C and 20 mT respectively. A total of 10 VGPs were obtained from radiometrically dated rocks (42–22 Ma); the averaged position (69°S, 334°E; α_{95}=9.9°) is the first middle Tertiary palaeomagnetic pole for East Antarctica, and gives evidence for a reversal in the course of the APW path. This evidence is not substantially altered by a supposed tilt-correction consistent with geophysical and geological models for the uplift of the Transantarctic Mountains. No definite conclusion about relative movements between East Antarctica and the Antarctic Peninsula can be drawn from the existing palaeomagnetic data.

Received 23 September 1994, accepted 31 July 1995

Key words: Tertiary, palaeomagnetism, palaeopole, Antarctica

Introduction

Palaeomagnetic data from East Antarctica are restricted to the Ordovician, Middle Jurassic and late Miocene–Holocene (Piper 1988, Lock & McElhinny 1991), with the result that its drift following separation from the other land masses of Gondwana has been mostly determined from analysis of sea-floor spreading magnetic anomalies (Embleton & McElhinny 1982, Lawver *et al.* 1985, Besse & Courtillot 1988, Livermore & Woollet, 1993) and to a lesser extent from seismic stratigraphy (Veevers & Eittreim 1988, Stagg & Willcox 1992). Additional results derived from continental palaeomagnetism would be useful to constrain better the drift history and establish a reference for comparing the drift of the various West Antarctica blocks.

Recent discovery of Tertiary plutons in the Transantarctic Mountains of northern Victoria Land (Stump *et al.* 1983, GANOVEX Team 1987) has provided an opportunity to draw a more detailed picture of the East Antarctica apparent polar wander (APW) path. A palaeomagnetic study was therefore planned as a part of the Italian Antarctic National Research Programme during the 1990/91 expedition.

Geological setting and sampling

The crystalline basement of northern Victoria Land is composed of metamorphic and igneous rocks deformed during the Cambro-Ordovician Ross orogeny, and cut by the Silurian-Devonian Kukri peneplain. Late Palaeozoic-Jurassic sedimentary and volcanic rocks rest unconformably on this peneplain. Northern Victoria Land was eventually affected by the Ross Sea rifting, which is thought to have begun as early as separation of Antarctica from Australia (Roland & Tessensohn 1987), and the uplift of the Transantarctic Mountains, which occurred over several episodes throughout the last 110 My (Fitzgerald & Gleadow 1988, Stump & Fitzgerald 1992) and was accompanied by alkaline magmatism. Late Miocene–Holocene volcanic rocks widespread along the Ross Sea coast, from Cape Adare to Mount Melbourne, were noted by the earliest explorers, whereas Tertiary intrusives were discovered only a few years ago (Stump *et al.* 1983). Subsequent fieldwork by German and Italian expeditions mapped the many intrusive bodies eventually grouped into the Meander Intrusives unit in the geological map drawn by the GANOVEX Team (1987). In our paper, we shall refer to this unit as including all the Tertiary plutons so far discovered in northern Victoria Land.

The Meander Intrusives are a series of small gabbro to granite stocks cropping out within a band roughly parallel to the Ross Sea coast, between the Campbell and Borchgrevink glaciers (Fig. 1). The K-Ar and Rb-Sr ages determined for many stocks (Armienti *et al.* 1990, Müller *et al.* 1991) range from 42 to 18 Ma, and decrease more or less regularly from south-west to north-east. According to Roland & Tessensohn (1987), the alignment of the stocks matches a regional structural axis, the Borchgrevink trend, along which NW tilting of the whole northern Victoria Land might have occurred during the uplift of the Transantarctic Mountains.

All the plutons reported in the literature were sampled, with the exception of that at Engberg Bluff. Moreover, a

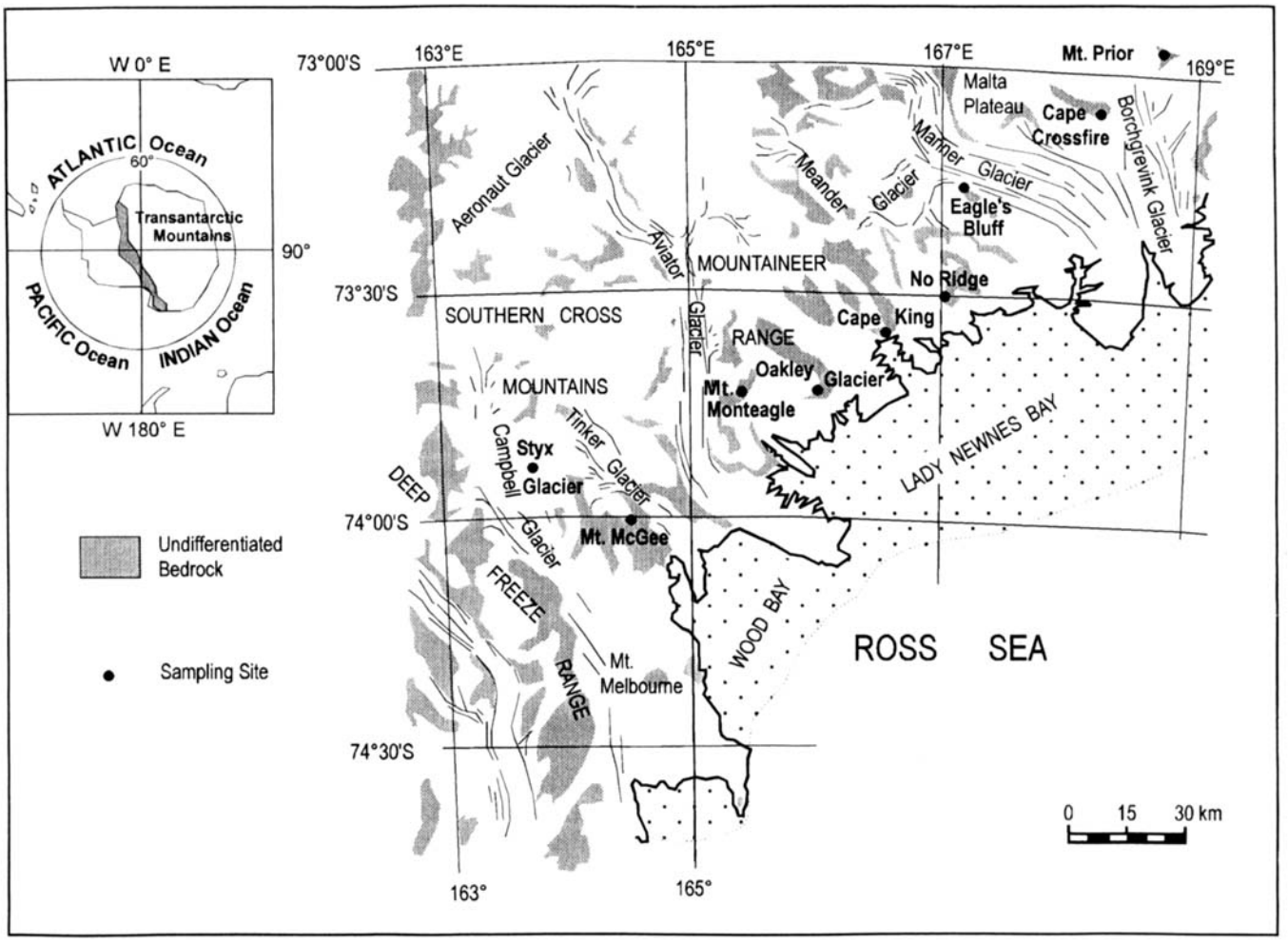

Fig. 1. Location of the study region and map of the sampling sites.

small gabbro body, discovered close to the Mount McGee monzonite stock and eventually dated at 38 ± 0.8 Ma (S. Tonarini, personal communication 1993), and the syenite cropping out at the head of Styx Glacier (Nathan 1971) were also sampled. The age of the syenite is unknown, but its signature on the aeromagnetic map (Bosum *et al.* 1989) is the same as that of the Meander Intrusives stocks. Small size and poor accessibility limited the number of sampling sites within some stocks. Four or five hand-samples were collected at each site, and oriented using both magnetic and sun compass. Three cores were cut from each sample and the routine magnetic measurements were done on one specimen from each core, giving a total of 12 or 15 specimens per site. Smaller total numbers were the result of sample or specimen break-up.

Magnetic mineralogy and remanent magnetization

Analytical methods

Thirty-two polished thin sections from selected samples were investigated by electron microscopy (SEM Cambridge S-360) and chemical analysis (EDS/SEM 2000 Link System; 15 kV and *c.* 400 pA). Standards were: SiO_2 for Si, TiO for Ti, Al_2O_3 for Al, Cr_2O_3 for Cr, haematite for Fe, Mn for Mn, MgO for Mg, wollastonite for Ca, NaCl for Na, KBr for K, Cu for Cu, NiO for Ni, barite for S. Data reduction was performed using the on-line ZAF programme (Duncumb & Reed 1968), and the analyses were recalculated with the NORM programme (Ulmer 1986). Table I reports the main mineralogical characteristics of each stock and Table II the results of the microprobe analyses of the Fe and Fe-Ti oxides. The oxides composition has been recalculated according to the scheme of Carmichael (1967). The oxide wt% total is often not equal, but very close to 100, because the small size of the intergrowth phases means that the volume analysed is not monomineralic (cf. Steinthorsson *et al.* 1992). TiO_2 wt% values have been used to group the oxides of the magnetite-ulvöspinel series in four classes, namely magnetite (0–0.1 wt%), low-Ti titanomagnetite (0.11–5.0), high-Ti titanomagnetite (5.01–18.0) and ulvöspinel (18.01–36) for the sole purpose of schematizing the relationships between ferromagnetic minerals and rock magnetic properties.

Magnetic susceptibility was measured with a Geofyzika

https://doi.org/10.1017/S0954102096000107 Published online by Cambridge University Press

Table I. Mineralogy of the Meander Intrusives stocks.

Site	Minerals	Opaque minerals	Types of intergrowth
Styx Glacier syenite	Kfs, Ab and Lbr-Byt, Hbl, Bt, OpM, Spn	Mag, low-Ti, high-Ti, Ilm > Usp, Ccp, Po	Ilm in low-Ti and high-Ti (with traces of Po) as sandwich type; Ilm in low-Ti and Mag as composite type
Mount McGee monzonite	Pl (Olg-And), Kfs, Qtz, Bt, Hd-Fs-Aug, green Hbl, Fa, OpM, Ap, Spn, Zrn, Rt, Prr, All	Mag, low-Ti, high-Ti, Usp, Ilm (Gt, Lm > Hem as alteration products)	Ilm in low-Ti as composite type > trellis and sandwich type
Mount McGee gabbro	Olg, Kfs, Aug, Pgt, Bt, green Hbl, OpM	low-Ti, high-Ti, Ilm, Py, Ccp, Po	Ilm in low-Ti and high-Ti as composite type
Mount Monteagle gabbro	Pl (Ab, Olg, And), Kfs, Aug-Fs, green Hbl, Bt, OpM, Ap, Spn, Zrn, Mnz	low-Ti, Ilm (with Po inclusions), Py (Gt as alteration)	
Mount Monteagle syenite	Kfs, Ab, Qtz, Ol, Hbl, Prx, Bt, OpM, Spn, Prc, Jcb	Gt, low-Ti, Hem, Lm	
Oakley Glacier monzonite	Kfs (mesoperthite and Ab-perthite), Qtz, Gru, Fs, Ap, Aln, OpM	Ilm, low-Ti (>Hem as alteration)	
Cape King gabbro	And, Qtz, green Hbl, Bt, Hps, OpM, Zrn, Spn	low-Ti, Usp, Ilm, Py, Ccp, Po, Gt and Hem as alteration	Usp in Ilm as lamellae; Ilm on Py and Ccp (Gt on Py and Ccp as curvilinear alteration)
No Ridge syenite	Kfs (perthite and meso perthite), Ab, Atl, Qtz, Hbl, Gru, Arf, Ang, Agr, OpM, Mnz	high-Ti, Mag, Ilm, Gt, Frg	Ilm in high-Ti as composite and sandwich type
Eagle's Bluff granite	Kfs (perthite and Ab-mesoperthite), Qtz, Bt, green Hbl, Zrn, OpM	high-Ti, low-Ti, Mag, Ilm (Hem as alteration)	Ilm in low-Ti as trellis type; Ilm in low-Ti and high-Ti as composite type
Cape Crossfire diorite	Pl (Ab + And), Hbl, OPrx, Bt, OpM	Ilm, high-Ti, low-Ti, Usp, Py (Hem and Gt as alteration)	Ilm in Usp, low-Ti, high-Ti as trellis type; Ilm in low-Ti as composite type
Mount Prior granite	Qtz, Kfs and Pl, Bt, Zrn, Rt, Mnz, OpM, Ptd, Aln	Ilm, low-Ti, high-Ti, Hem, Lm	

Symbols for minerals according to Kretz (1983), plus: aegirina = Agr, aenigmatite = Ang, andesina = And, anorthoclase = Atl, bytownite = Byt, fergusonite = Frg, hyperstene = Hps, jacobsite = Jcb, labradorite = Lbr, oligoclase = Olg, opaque minerals = OpM, orthopyroxene = Oprx, perrierite = Prr, portlandite = Ptd, pyrochlore = Prc, pyroxene = prx.

KLY-2 bridge, and natural remanent magnetization (NRM) with a JR-4 spinner magnetometer. Four pilot specimens from each site were stepwise demagnetized, two in alternating field (AF) and two thermally. Susceptibility was measured after each thermal step to detect heat-induced mineralogical transformations. The procedure most effective for each site was used to demagnetize the remaining specimens through four to seven steps, and the characteristic remanent magnetization (ChRM) direction was then calculated by linear interpolation. The isothermal remanence (IRM) was investigated using a pulse magnet with a maximum field of 1.5 T. The main magnetic results are presented in Table III.

The mineralogical and magnetic data are discussed separately for each of the stocks, owing to the variations in their individual characteristics.

Styx Glacier

A rather altered syenite of unknown age crops out along the southern ridge of the hill (spot height 1890) at the head of Styx Glacier (Nathan 1971). The normalized intensity decay curve during thermal demagnetization shows a sharp decrease between 200 and 350°C (A in Fig. 2). At higher temperatures, the intensity continues to decrease and is completely removed below 600°C. These results are consistent with the presence of magnetite and both low- and high-Ti titanomagnetite. IRM saturation was reached at a field value H_S = 0.2 T and the remanent coercive force was H_{RC} = 50 mT. The NRM was widely scattered and always of reverse polarity. Thermal demagnetization removed secondary magnetization components within 200°C; thereafter, the direction did not change up to the higher Curie point. The same direction stability was found during AF demagnetization above 20 mT (Fig. 3a). AF demagnetization in the range 20–60 mT was used to isolate the ChRM of all specimens, and greatly reduced the directional scattering.

Mount McGee

A monzonite stock is well exposed on the northern slopes of Mount McGee (sites 1–4). The Rb-Sr age (whole-rock biotite pair) is 37.9 ± 1.1 Ma (Armienti *et al.* 1990). The magnetization intensity decays steadily throughout thermal demagnetization and the normalized curve does not show a

https://doi.org/10.1017/S0954102096000107 Published online by Cambridge University Press

Table II. Electron microprobe analyses of Fe and Fe-Ti oxides from the Meander Intrusives.
Symbols: Ilm = ilmenite; Mag, low-Ti, high-Ti, Usp = magnetite, low- and high-Ti titanomagnetite, ulvöspinel (see text for explanation); Hem = haematite. Italic figures in parentheses = number of averaged analyses. Oxide values in wt%; iron measured as total FeO; Fe_2O_3 calculated with the NORM program (Ulmer 1986); end-member per cent values obtained according to Carmichael (1967).

	Ilm	Mag	low-Ti	high-Ti	Usp	Hem		Ilm	Mag	low-Ti	high-Ti	Usp	Hem
Styx Glacier	*(5)*	*(3)*	*(3)*	*(2)*	*(1)*		Oakley Glacier	*(16)*		*(2)*			*(4)*
SiO_2	0.43	–	–	–	0.50	–	SiO_2	–	–	1.25	–	–	1.09
TiO_2	51.85	–	2.02	8.05	34.94	–	TiO_2	51.52	–	0.59	–	–	–
Al_2O_3	–	–	–	–	–	–	Al_2O_3	–	–	–	–	–	–
FeO	43.73	90.09	88.54	82.95	60.63	–	FeO	41.45	–	89.31	–	–	86.16
MnO	2.83	–	–	–	2.38	–	MnO	5.65	–	–	–	–	–
Total	99.34	90.09	90.56	90.99	98.45	–	Total	98.62	–	91.15	–	–	87.25
FeO	43.73	30.03	31.94	37.30	60.63	–	FeO	40.61	–	32.47	–	–	1.30
Fe_2O_3	0.00	66.74	62.90	50.73	–	–	Fe_2O_3	0.94	–	63.16	–	–	94.30
Total	98.84	96.77	96.86	96.08	98.45	–	Total	98.71	–	97.47	–	–	96.69
Mag%	–	100.0	94.0	75.9	0.0	–	Mag%	–	–	98.9	–	–	–
Usp%	–	–	6.0	24.1	99.2	–	Usp%	–	–	1.7	–	–	–
Ilm%	93.4	–	–	–	–	–	Ilm%	86.9	–	–	–	–	–
Hem%	–	–	–	–	–	–	Hem%	–	–	–	–	–	100.0
Mount McGee 1–4	*(56)*	*(5)*	*(28)*	*(2)*	*(1)*	*(3)*	Cape King 1–3	*(53)*		*(18)*		*(2)*	*(4)*
SiO_2	–	1.64	–	–	–	–	SiO_2	–	–	–	–	–	–
TiO_2	51.27	–	1.68	5.78	18.44	1.38	TiO_2	48.75	–	1.62	–	25.46	0.53
Al_2O_3	–	–	–	–	–	0.46	Al_2O_3	–	–	0.98	–	–	0.38
FeO	45.61	91.28	91.21	89.99	75.51	85.62	FeO	47.76	–	89.75	–	68.77	87.89
MnO	2.24	–	–	–	1.26	–	MnO	1.11	–	–	–	0.46	–
Total	99.12	92.92	92.90	95.77	95.21	87.46	Total	97.62	–	92.35	–	94.69	88.81
FeO	43.84	33.04	32.42	36.57	46.43	1.24	FeO	42.71	–	32.32	–	53.14	0.48
Fe_2O_3	1.97	64.72	65.33	58.39	32.32	93.77	Fe_2O_3	5.61	–	63.82	–	17.37	97.14
Total	99.32	99.40	99.43	100.67	98.45	96.85	Total	98.18	–	98.74	–	96.43	98.53
Mag%	–	100.0	95.1	83.6	42.6	–	Mag%	–	–	93.0	–	23.9	–
Usp%	–	–	4.9	16.4	53.3	–	Usp%	–	–	4.7	–	74.6	–
Ilm%	93.3	–	–	–	–	–	Ilm%	92.1	–	–	–	–	–
Hem%	–	–	–	–	–	96.4	Hem%	–	–	–	–	–	98.3
Mount McGee 5	*(33)*		*(3)*	*(1)*		*(2)*	No Ridge 1–2	*(13)*	*(4)*		*(4)*		
SiO_2	–	–	–	–	–	–	SiO_2	–	–	–	–	–	–
TiO_2	50.66	–	1.67	7.25	–	1.00	TiO_2	52.49	–	–	12.79	–	–
Al_2O_3	–	–	1.15	–	–	0.83	Al_2O_3	–	–	–	–	–	–
FeO	44.95	–	89.94	80.41	–	86.78	FeO	38.66	90.60	–	79.11	–	–
MnO	1.44	–	–	–	–	–	MnO	7.52	–	–	1.04	–	–
Total	97.05	–	92.76	91.68	–	88.61	Total	98.67	90.60	–	92.94	–	–
FeO	44.10	–	32.52	35.50	–	0.90	FeO	38.66	30.20	–	41.00	–	–
Fe_2O_3	–	–	63.81	49.91	–	95.44	Fe_2O_3	–	67.12	–	42.35	–	–
Total	97.14	–	99.15	92.66	–	98.17	Total	98.67	97.32	–	97.18	–	–
Mag%	–	–	92.5	77.5	–	–	Mag%	–	100.0	–	58.9	–	–
Usp%	–	–	4.8	22.5	–	–	Usp%	–	–	–	37.6	–	–
Ilm%	95.9	–	–	–	–	–	Ilm%	84.4	–	–	–	–	–
Hem%	–	–	–	–	–	96.7	Hem%	–	–	–	–	–	–

clear decrease at the passing of the Curie point of the high-Ti titanomagnetite (B in Fig. 2). Together with the low values of H_S (0.1 T) and H_{RC} (≤ 20 mT), this suggests that most of the ferromagnetic grains are multidomain. The Zijderveld graphs show that temperature values higher than 400°C are needed to separate a stable component (Fig. 3f), which is probably carried by the smallest magnetite and low-Ti titanomagnetite grains. All specimens were demagnetized at four steps, between 400 and 520°C. Demagnetization was not successful at site 2 where the NRM mean direction (D = 143°, I = -81°) is very close to the present field (D = 137°, I = -83°), and points to the predominance of viscous, unstable

https://doi.org/10.1017/S0954102096000107 Published online by Cambridge University Press

Table II. Continued.

	Ilm	Mag	low-Ti	high-Ti	Usp	Hem		Ilm	Mag	low-Ti	high-Ti	Usp	Hem
Mount McGee dyke	*(13)*	*(5)*	*(1)*	*(1)*	*(1)*	*(1)*	Eagle's Bluff 1-3	*(5)*	*(1)*	*(8)*	*(5)*		*(2)*
SiO_2	–	1.03	0.70	3.66	–	0.37	SiO_2	–	1.80	–	–	–	–
TiO_2	49.34	–	0.54	11.56	25.26	0.68	TiO_2	49.77	–	1.74	8.09	–	0.98
Al_2O_3	–	–	–	1.03	–	0.38	Al_2O_3	–	–	–	–	–	–
FeO	47.76	89.03	83.93	75.24	69.16	85.41	FeO	38.06	88.59	89.42	85.11	–	85.71
MnO	2.25	–	–	0.47	0.98	–	MnO	11.77	–	–	–	–	–
Total	99.35	90.36	91.97	91.96	95.40	86.84	Total	99.60	90.39	91.16	93.20	–	86.68
FeO	42.09	31.32	29.74	44.94	52.68	1.05	FeO	32.83	32.40	31.89	38.07	–	0.88
Fe_2O_3	6.30	64.13	60.22	33.67	18.32	93.74	Fe_2O_3	5.81	62.44	63.93	52.27	–	94.27
Total	99.98	96.48	91.20	95.33	97.23	96.23	Total	100.18	96.64	97.56	98.43	–	96.13
Mag%	–	100.0	98.2	56.6	23.4	–	Mag%	–	100.0	94.8	76.4	–	–
Usp%	–	–	1.7	33.9	73.4	–	Usp%	–	–	5.2	23.6	–	–
Ilm%	89.2	–	–	–	–	–	Ilm%	69.3	–	–	–	–	–
Hem%	–	–	–	–	–	98.0	Hem%	–	–	–	–	–	98.0
Mount Monteagle 1			*(7)*			*(2)*	Cape Crossfire	*(16)*		*(12)*	*(12)*	*(12)*	*(6)*
SiO_2	–	–	–	–	–	–	SiO_2	–	–	–	–	–	–
TiO_2	–	–	2.15	–	–	1.41	TiO_2	51.00	–	2.35	11.40	25.10	0.69
Al_2O_3	–	–	–	–	–	–	Al_2O_3	–	–	–	–	–	–
FeO	–	–	89.85	–	–	85.49	FeO	45.30	–	87.84	76.35	65.64	88.24
MnO	–	–	–	–	–	–	MnO	2.49	–	–	–	1.20	–
Total	–	–	92.00	–	–	86.90	Total	98.79	–	90.19	87.75	91.94	88.93
FeO	–	–	32.53	–	–	1.27	FeO	43.34	–	32.10	39.12	51.16	0.62
Fe_2O_3	–	–	63.70	–	–	93.59	Fe_2O_3	2.18	–	61.94	41.37	16.09	97.37
Total	–	–	98.38	–	–	96.27	Total	99.01	–	96.39	91.89	93.55	98.68
Mag%	–	–	93.7	–	–	–	Mag%	–	–	93.0	64.5	20.2	–
Usp%	–	–	6.3	–	–	–	Usp%	–	–	7.0	35.5	75.7	–
Ilm%	–	–	–	–	–	–	Ilm%	92.5	–	–	–	–	–
Hem%	–	–	–	–	–	97.1	Hem%	–	–	–	–	–	98.6
Mount Monteagle 2-3	*(19)*		*(2)*				Mount Prior			*(1)*	*(1)*		
SiO_2	–	–	–	–	–	–	SiO_2	–	–	2.43	–	–	–
TiO_2	49.62	–	0.97	–	–	–	TiO_2	–	–	3.36	16.68	–	–
Al_2O_3	–	–	–	–	–	–	Al_2O_3	–	–	3.13	1.39	–	–
FeO	44.71	–	91.38	–	–	–	FeO	–	–	85.90	76.41	–	–
MnO	1.19	–	–	–	–	–	MnO	–	–	–	–	–	–
Total	95.52	–	92.35	–	–	–	Total	–	–	94.82	94.48	–	–
FeO	43.42	–	31.62	–	–	–	FeO	–	–	38.01	46.12	–	–
Fe_2O_3	1.44	–	66.41	–	–	–	Fe_2O_3	–	–	53.22	33.66	–	–
Total	95.66	–	99.00	–	–	–	Total	–	–	100.15	97.85	–	–
Mag%	–	–	97.2	–	–	–	Mag%	–	–	82.1	48.7	–	–
Usp%	–	–	2.8	–	–	–	Usp%	–	–	9.4	48.2	–	–
Ilm%	95.9	–	–	–	–	–	Ilm%	–	–	–	–	–	–
Hem%	–	–	–	–	–	–	Hem%	–	–	–	–	–	–

magnetization.

The monzonite stock crops out along the western side of a tributary valley of Tinker Glacier; on the eastern side, a small gabbro stock was discovered and sampled (site 5). The whole-rock biotite Rb-Sr age (38 ± 0.8 Ma, (S. Tonarini, personal communication 1993) is the same as the main stock. Low-Ti titanomagnetite is the main ferromagnetic mineral, because only a small fraction of the initial NRM was removed by thermal demagnetization below about 520°C. Weak secondary components aligned with the present field were easily removed by thermal or AF demagnetization (Fig. 3b), both of which showed a good directional stability up to the higher steps. The ChRM direction was computed after AF cleaning between 20 and 40 mT.

The Mount McGee stock is cut by several vertical dykes. One was sampled and its composition proved to be similar to

https://doi.org/10.1017/S0954102096000107 Published online by Cambridge University Press

Table III. Site-average palaeomagnetic data for the Meander Intrusives.

Site		Lith.	Age	Coordinates		N/n	k_m	J_r	NRM			ChRM				VGP		Demagnetization
			Ma	Lat. S	Long. E		$\times 10^{-6}$ SI	A/m	D	I	α_{95}	D	I	k	α_{95}	Lat. S	Long. E	
Styx Glacier		S	?	73.9	163.7	10/10	14738	0.31	118.9	+36.8	25.1	115.2	+47.7	41	7.6	34	270	AF 20–60 mT
Mt. McGee	1	M	38	74.0	164.5	15/15	14090	0.19	19.7	-78.5	16.9	346.2	-61.7	67	6.4	58	325	Th 400–520 °C
	2	M	"	"	"	9	39735	0.50	142.9	-80.5	22.4		unstable			–	–	Th 400–520 °C
	3	M	"	"	"	11/11	26645	1.22		scattered		357.9	-45.5	31	10.1	43	342	Th 400–520 °C
	4	M	"	"	"	12/12	15682	0.35	276.1	-83.7	22.9	335.8	-76.8	9	15.9	78	290	Th 400–520 °C
	5	Ga	38	74.0	164.6	15/15	29495	1.53	22.2	-85.8	4.6	335.8	-70.4	254	2.9	68	305	AF 20–40 mT
Mt. McGee dyke		M	< 38	74.0	164.5	8/8	54931	2.86		scattered		8.1	-68.6	28	10.7	68	358	AF 40 mT
Mt. Monteagle	1	S	< 42	73.7	165.5	12	5998	1.67		scattered			scattered			–	–	Th 400–560 °C
	2	Ga	42	"	"	15/15	538	0.01	194.5	+81.5	6.4	161.8	+76.5	99	4.4	79	302	Th 480–545 °C
	3	Ga	"	"	"	12/6	4547	0.95		scattered		181.5	+80.1	482	3.1	–	–	Th 530–580 °C
Oakley Glacier		M	Tertiary	73.7	166.0	12/12	13497	0.70		scattered		130.8	+67.0	96	4.4	58	277	Th 400–560 °C
Cape King	1	Ga	28	73.6	166.6	11	72065	3.75		scattered			unstable			–	–	Th 360–540 °C
	2	Ga	"	"	"	12/12	2692	0.14	151.4	+60.2	17.5	165.4	+69.4	68	5.9	69	322	Th 360–540 °C
	3	Ga	"	"	"	14/14	1274	0.02		scattered		210.0	+69.7	76	5.3	66	35	Th 360–540 °C
No Ridge	1	S	26	73.5	167.0	12	1264	0.09	287.3	+35.4	17.3		scattered			–	–	AF 30–60 mT
	2	S	"	"	"	12/12	3108	0.04		scattered		342.1	-77.8	105	4.7	81	297	AF 30–60 mT
Eagle's Bluff	1	G	24	73.3	167.2	15/15	5102	0.03		scattered		167.4	+68.9	27	10.1	68	326	AF 20–50 mT
	2	G	"	"	"	15/15	3259	0.02		scattered		192.7	+60.3	23	9.2	57	5	Th 440–560 °C
	3	G	"	"	"	15	8175	0.05		scattered			unstable			–	–	Th 400–560 °C
C. Crossfire		D	Tertiary	73.1	168.2	9/9	47870	2.49	312.7	-70.4	16.6	337.5	-72.3	336	2.8	72	306	AF 20–30 mT
Mt. Prior		G	19	72.9	168.8	15	1856	0.16		scattered			unstable			–	–	Th 300–560 °C

Abbreviations: S = syenite; M = monzonite; Ga = gabbro; G = granite; D = diorite; N/n = number of specimens collected/used for calculating the mean ChRM direction; k_m = bulk susceptibility; J_r = NRM intensity; NRM = natural remanent magnetization; D = declination; I = inclination; α_{95} = semi-angle of confidence; ChRM = characteristic remanent magnetization after demagnetization; k = Fisher's precision parameter; VGP = southern virtual geomagnetic pole; Demagnetization = minimum and maximum peak-field or temperature using either AF or thermal technique. Scattered = resultant vector R less than significance point R_0; unstable = no stable component isolated by demagnetization.

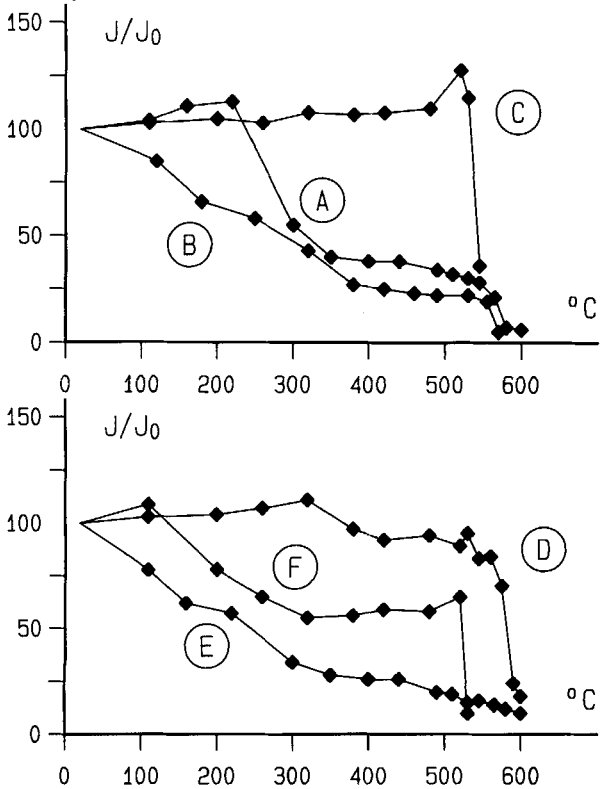

Fig. 2. Normalized intensity decay curves for thermal demagnetization. A = Styx Glacier syenite, B = Mount McGee monzonite, C = Mount Monteagle gabbro, D = Cape King gabbro, E = No Ridge syenite, F = Cape Crossfire dyke.

that of the monzonite. The NRM directions were widely scattered, because of large secondary components. These were removed either at temperatures higher than 400°C or at peak-field values greater than 30 mT. AF demagnetization at 40 mT was used to isolate the ChRM.

Mount Monteagle

The top of Mount Monteagle consists of gabbro and syenite. The whole-rock biotite Rb-Sr age of the gabbro is 42 ± 0.8 Ma (S. Tonarini, personal communication 1993), and small gabbro inclusions give evidence for a younger age of the syenite. The magnetic properties of the gabbro (sites 2 & 3) are mainly those of low-Ti titanomagnetite (Curie point *c.* 540°C, H_s = 0.2 T and H_{RC} = 45 mT), with the exception of some specimens that only approach saturation at the highest available field (1.5 T) and are likely to have a higher goethite content. The NRM directions at site 2 are well clustered and all of reverse polarity. The magnetization is very stable and the blocking temperature spectrum ranges from 480 to 520°C to the Curie point (C in Fig. 2). The ChRM direction was derived through thermal demagnetization at four steps between 480 and 545°C (Fig. 3g). The NRM directions from site 3 are widely scattered. AF and thermal demagnetization pointed to the occurrence of two components of opposite polarity. Unfortunately, the coercivity and blocking temperature spectra of the two components often overlapped. Remagnetization circle analysis was successful for only six

https://doi.org/10.1017/S0954102096000107 Published online by Cambridge University Press

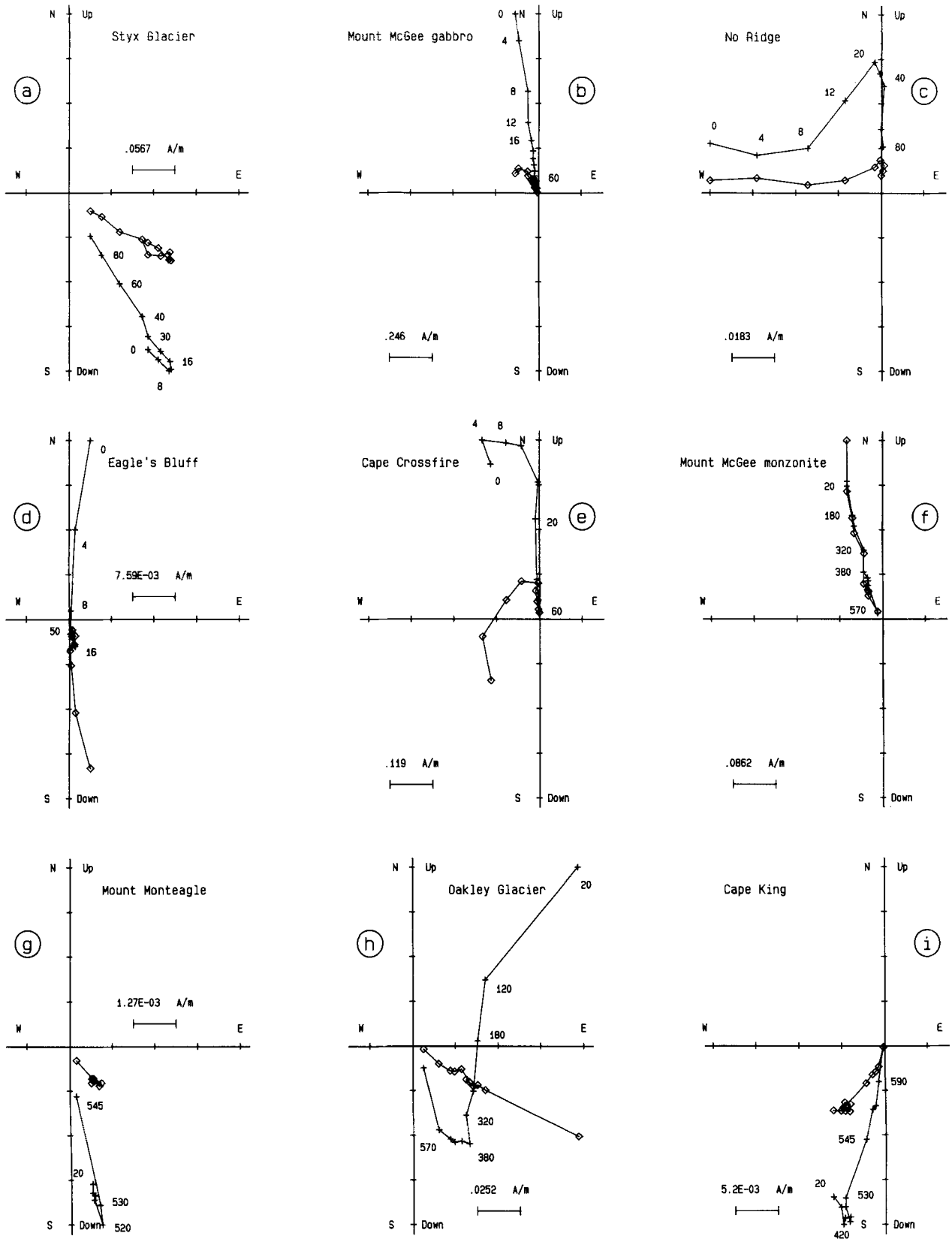

Fig. 3. Zijderveld diagrams for AF (**a, b, c, d, e**) and thermal (**f, g, h, i**) demagnetization. Open squares = declination, crosses = apparent inclination, figures = peak-field (mT) or temperature (°C) value.

https://doi.org/10.1017/S0954102096000107 Published online by Cambridge University Press

specimens, and gave a reverse direction similar to that of site 2. As the number of specimens was only 50% of the total, this site was not taken further into consideration.

The blocking temperature spectrum of the syenite (site 1) ranges from room temperature to *c.* 560°C, with no substantial changes in the magnetization direction. The directions for the specimens from the same hand-sample are similar, whereas from one sample to another they only share declinations within the southern quadrants, and no significant mean value could be calculated.

Oakley Glacier

This stock was briefly described by Müller *et al.* (1991), but no radiometric age is available. It is difficult of access, because it crops out along the steep walls of the southern side of Oakley Glacier valley. Samples were collected from the southern divide, and consist of an altered monzonite. The magnetic properties are consistent with the occurrence of low-Ti titanomagnetite as the main ferromagnetic mineral: H_S = 0.2 T, H_{RC} = 20 mT, and at least 95% of the NRM intensity was removed by thermal demagnetization up to 580°C. The demagnetization diagrams show the occurrence of a large secondary magnetization component, removed by 400°C, and a more stable component, whose direction is of reverse polarity and stable at the higher temperatures (Fig. 3h). Thermal demagnetization between 400 and 560°C was used to isolate the ChRM, and greatly reduced the within-site scattering.

Cape King

A gabbro stock was sampled at the top of the cliffs, along the plateau where a weather antenna is located. Armienti *et al.* (1990) reported a whole-rock biotite Rb-Sr age of 28.1 ± 0.8 Ma. No mineralogical differences were detected between site 1 and sites 2 and 3, and the rock magnetic properties are, on the whole, similar to those of the gabbro from Mount Monteagle. Site 1 is characterized by a great titanomagnetite content, which results in a very high susceptibility value and large secondary magnetizations. The NRM directions are widely scattered and the demagnetization procedures failed to isolate any stable component. At sites 2 and 3, on the other hand, the magnetization withstood temperatures up to about 500°C (D in Fig. 2), and secondary components are weak and easily removed by thermal demagnetization (Fig. 3i). The ChRM of each specimen was determined after five heating steps in the range 360–540°C, and was always of reverse polarity.

No Ridge

The stock on the western side of Suter Glacier valley consists of an altered syenite and has yielded two K-Ar ages of 25.7 ± 0.3 and 26.0 ± 0.5 Ma (Müller *et al.* 1991). The curve of intensity decay (E in Fig. 2) shows that a temperature of *c.* 400°C is enough to remove 75% of the initial NRM, probably because of the low Curie point of the high-Ti titanomagnetite. The IRM saturation field was H_S = 0.2 T, and the remanent coercive force H_{RC} = 40 mT. AF (Fig. 3c) was more effective than thermal demagnetization and all specimens were demagnetized in the peak-field range 30–60 mT. The resulting ChRM directions were well clustered at site 2, and scattered at site 1.

Eagle's Bluff

The stock located at the confluence of the Meander and Mariner glaciers is the first Tertiary intrusion to have been discovered in northern Victoria Land (Stump *et al.* 1983). It was fully described by Müller *et al.* (1991), who also gave Rb-Sr and K-Ar ages ranging from 22 to 25 Ma. The IRM saturation field value was H_S = 0.15 T, and the remanent coercive force H_{RC} = 30 mT. Large secondary magnetization components of normal polarity screen a reverse stable component. They were removed by AF demagnetization at peak-field values greater than 20 mT at site 1 (Fig. 3d), and by thermal demagnetization at temperatures higher than 400°C at site 2. The weak magnetization persisting at temperatures higher than 600°C may be due to heat-induced oxidation, because it was matched by a regular decrease in the susceptibility measured after each heating step. At site 3, both thermal and AF demagnetization failed to isolate any stable component.

Cape Crossfire

Granite and dykes crop out along the south-eastern ridge of the unnamed mountain (spot height 2080) north-north-west of Cape Crossfire. The rocks are commonly deeply altered and the opaque minerals content is small. Susceptibility values are very low (< 500 x 10^{-6} SI) and the magnetization is weak and unstable, with the exception of a dioritic dyke, which is the only one discussed here. The IRM parameters are similar to those derived from the Eagle's Bluff granite. More than 50% of the NRM is carried by the low-Ti titanomagnetite, as shown by the intensity decay curve during thermal demagnetization (F in Fig. 2). Both thermal and AF (Fig. 3e) demagnetization were effective in isolating the ChRM, and the specimens were AF demagnetized at four steps between 20 and 40 mT.

Mount Prior

The northernmost of the Meander Intrusives stocks crops out between Borchgrevink and Whitehall glaciers. It is also the youngest, with a K-Ar age of 18.7 ± 0.3 Ma (Müller *et al.* 1991). The NRM directions were widely scattered, all characterized by positive inclination. Both thermal and AF demagnetization failed to isolate a stable component. Erratic

changes of declination were observed during demagnetization, whereas the inclination was low and positive (30–50°).

Remarks

Electron microprobe microanalysis identified several opaque minerals: ilmenite, magnetite-ulvöspinel, haematite, goethite, limonite, pyrrhotite, pyrite, chalcopyrite. Low-Ti titanomagnetite and ilmenite occur in greatest amounts and in nearly all samples. The content, if any, of ulvöspinel and sulphides is everywhere very low. Haematite, goethite and limonite are common as alteration products. The habit of the ilmenite crystals is mostly roundish, at times hexagonal. The composition of ilmenite from the different stocks is rather homogeneous, with a MnO weight-content of about 2%. This value corresponds to crystallization temperatures of 600–800°C. On the other hand, the MnO content increases up to 12% in the ilmenite from the Oakley Glacier, No Ridge and Eagle's Bluff stocks. According to Haggerty (1976b), such a high value is typical of peralkaline suites and points to a crystallization temperature <500°C. Low-Ti titanomagnetite is the most common spinel, and occurs as irregular, skeleton or polygonal crystals, often included within the silicates, mainly biotite. High-Ti titanomagnetite and ulvöspinel grains are roundish. It is worth noting that the composition of the ulvöspinel from the Styx Glacier stock is very close to the end member Fe_2TiO_4, which has so far been reported only in some Queensland rhyolites (Ewart *et al.* 1977) and lunar basalts (Deer *et al.* 1992).

Subsolidus reaction structures are widespread in the rocks of the Styx Glacier, Mount McGee, Cape King, No Ridge, Eagle's Bluff and Cape Crossfire sites. In most cases, they occur as oxidation exsolution of magnetite *s.l.* to ilmenite. The composite type is prevalent with respect to the trellis and sandwich types, and typically occurs in low-Ti titanomagnetite. The width of the ilmenite lamellae is typically < 10 μm in the composite and trellis structure, and rises to ≈100 μm in the sandwich type. In this particular case, magnetite *s.l.* has nucleated upon primary ilmenite. In the trellis structures, the ilmenite lamellae occur along the {111} cubic spinel planes. They result from primary oxidation (C2 stage of Haggerty 1976a) and point to crystallization temperatures between 600 and 800°C. Reduction exsolution structures were only observed in the Cape King gabbro and Cape Crossfire dyke. They consist of large ilmenite grains, including lamellae of magnetite *s.s.* along the {0001} rhombohedral planes. The reduction hypothesis is supported by the concomitant occurrence of pyrite related to the hydrothermal activity (Haggerty 1991).

The NRM directions of the Meander Intrusives are widely scattered, as the α_{95} value was less than 16° at two sites only and the resultant vector R less than the significance point R_0 of the Fisher statistics at twelve sites (Table III). Thermal and AF demagnetization showed that the dispersion is caused by widespread secondary components, which were usually

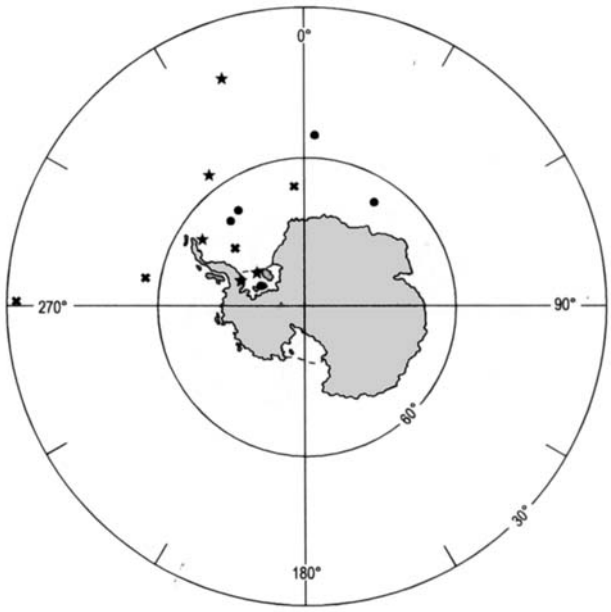

Fig. 4. VGP positions from the Meander Intrusives of northern Victoria Land. Symbols according to rock age: stars = late Eocene (Mount Monteagle, Mount McGee), circles = late Oligocene (Cape King, No Ridge, Eagle's Bluff), crosses = no radiometric age available (Styx Glacier = undated, Oakley Glacier = Tertiary, Mount McGee dyke < 38 Ma, Cape Crossfire dyke = Tertiary).

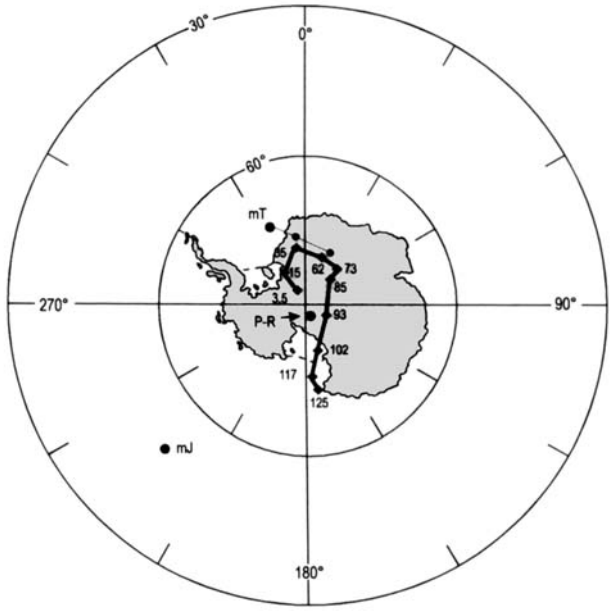

Fig. 5. Mesozoic to Recent palaeomagnetic data for East Antarctica. Large dots = palaeopoles: mJ = middle Jurassic, ~174 Ma (Lanza & Zanella 1993); mT = Middle Tertiary, 42–22 Ma (this paper); P-R = Pliocene to Recent, 5–0 Ma (Mankinen & Cox 1987). Thick line = 125–3.5 Ma synthetic APW path (DiVenere *et al.* 1994). Small dots = middle Tertiary palaeopole from the Meander Intrusives corrected for a 5° and 10° north-westerly tilt about the N45°E axis.

https://doi.org/10.1017/S0954102096000107 Published online by Cambridge University Press

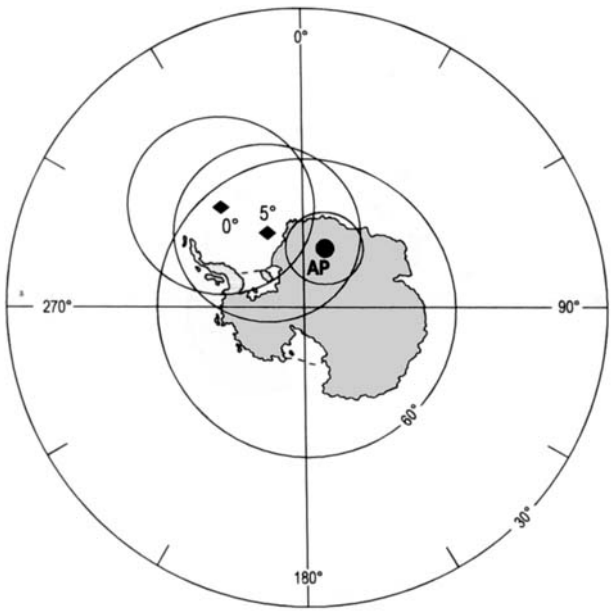

Fig. 6. Early Eocene palaeopole (AP) from the Antarctic Peninsula (Grunow 1993) and late Eocene palaeopole from the Meander Intrusives before (0°) and after (5°) the correction for north-westerly tilt about the N45°E axis.

removed at temperatures higher than 300–400°C or peak-field values greater than 20 mT. Fourteen of the 21 sites investigated gave a significant site mean ChRM direction, regarded as primary on the grounds of the mineralogical and magnetic characteristics. Half the directions are normal and half reverse; the reverse polarity of Mount Monteagle (42.0 ± 0.8 Ma) and the normal of Mount McGee (37.9 ± 1.1 Ma) agree well with the prevailing polarity of anomalies 19 (42.6–41.3 Ma) and 17 (38.5–36.7 Ma) respectively (Cande & Kent 1992), whereas the high reversal rate within anomalies 6A to 9 prevents significant comparison with Eagle's Bluff, No Ridge and Cape King.

Discussion

Fourteen of the 21 sampled sites gave a statistically significant site mean ChRM direction, which was used to calculate the position of the southern virtual geomagnetic pole (VGP) (Table III & Fig. 4). Most VGPs fall in the 270°E–360°E longitude quadrant and their latitudes range from 34°S to 81°S. We note first that the VGP from the Styx Glacier syenite (34°S, 270°E) is quite different from the others. We exclude it from further consideration, both because the rock age is unknown and because its very limited exposure along a snowy ridge prevented structural observation in the field. Nothwithstanding the field evidence for a Tertiary age, we also left out the VGPs from Oakley Glacier and the dykes of Mount McGee and Cape Crossfire, because they lack radiometric determination. The mean location of the remaining 10 VGPs (69°S, 334°E; $\alpha_{95} = 9.9°$) is the Meander Intrusives palaeopole averaged over the time span from 42–22 Ma.

This is the first middle Tertiary palaeomagnetic pole from East Antarctica, and its significance must first be assessed with respect to the APW path. The Mesozoic to Recent East Antarctica APW path relies on only two data points from East Antarctica itself (Fig. 5): the Middle Jurassic and the late Pliocene to Recent palaeopoles, derived from the Ferrar dolerite (Lanza & Zanella 1993) and the volcanic rocks of the Ross Sea margin (Mankinen & Cox 1988), respectively. The APW path or single palaeopoles for selected ages between ~174 Ma and 5–0 Ma have therefore been calculated by rotating palaeopoles from other continents into the East Antarctica reference frame using a variety of data sets, pole selection standards, timescales and rotation parameters. A full analysis of the results thus obtained is beyond the aim of this paper. We shall simply refer to the most up-to-date synthetic APW path from 125 to 3.5 Ma (DiVenere *et al.* 1994). The Tertiary part is based on African poles (Schneider & Kent 1990, Tauxe *et al.* 1983) rotated to Antarctica according the reconstructions of Mayes *et al.* (1990) and Royer *et al.* (1988). The palaeopole (Fig. 5) was close to the geographic South Pole at about 90 Ma, moved towards Dronning Maud Land in the Late Cretaceous, reversed its course in the Tertiary and then moved back towards the South Pole. The 42–22 Ma palaeopole from the Meander Intrusives falls not far from the middle Tertiary portion of the synthetic path and strengthens the evidence that the APW path reversed its course.

The gap between the new palaeopole position and the synthetic path might be the result of a post-emplacement tilting of the stocks, which would have altered the palaeomagnetic directions. Late Mesozoic to Recent tectonics strongly affected the whole of northern Victoria Land. Their most spectacular result was the uplift of the Transantarctic Mountains, of the order of 5–10 km in the coastal region facing the Ross Sea (Fitzgerald & Gleadow 1988). In southern Victoria Land, the uplift is thought to have caused the regional westward dip of the Kukri peneplain (Stern & ten Brink 1989). The Meander Intrusives unfortunately crop out in an area where direct evidence for tilting is lacking, because neither the Kukri peneplain nor its sedimentary cover has been preserved from erosion. However, north-westerly tilting of the whole of northern Victoria Land has been proposed by Roland & Tessensohn (1987), who regarded the Borchgrevink Coast as the trace of a major fault or flexure.

The rock fabric of the Meander Intrusives stocks does not show clear structural markers to infer their original attitude and no information could be derived from the outcrops. In the absence of field data, we tested the hypothesis of a north-westerly tilting of northern Victoria Land suggested by Roland & Tessensohn (1987). The mean site ChRM directions were therefore corrected at two rotation steps (5° and 10°) for a north-westerly tilt around the N45°E axis, and the corresponding new VGPs were calculated, together with the

new palaeopole. The tilt correction did not significantly alter the VGPs dispersion, for the difference between the α_{95} values before and after the correction was always ≤1°. The results of this exercise are summarized in Fig. 5, which shows that the supposed tilting brings the Meander Intrusives palaeopole closer to the synthetic APW path. The corrected palaeopoles are 75°S, 352°E with α_{95} = 10.4° for tilt angles of 5°, and 78°S, 27°E with α_{95} = 10.9° for angles of 10°. We may therefore conclude that the north-westerly tilting of northern Victoria Land, suggested by geophysical (Stern & ten Brink 1989) and geological (Roland & Tessensohn 1987) models as a consequence of the flexural uplift of the Transantarctic Mountains, would shorten the gap between the 42–22 Ma palaeopole from the Meander Intrusives and the corresponding portion of the synthetic APW path, and would not substantially alter the evidence for an early Tertiary reversal in the path. In our theoretical exercise, we assumed that each single block turned through the same angle and along the same direction, whereas a more realistic model would be a mosaic of differentially tilted blocks (Fitzgerald & Gleadow 1988), as observed in the central and western parts of Victoria Land, where the westerly dips of the Kukri peneplain range from horizontal to 10° (Walker 1983, Fitzgerald & Gleadow 1988). The existing data, however, are not enough to allow a more precise quantification of the tilt hypothesis.

Tertiary palaeomagnetic data from West Antarctica have long been available (Blundell 1962, Dalziel *et al.* 1973, Valencio *et al.* 1979, Watts *et al.* 1986, Grunow 1993). The results come from Palaeocene to early Eocene volcanic and intrusive rocks from the Antarctic Peninsula; some lack radiometric age determination and many lack a sound evaluation of the possibility of local tectonic movements. Grunow (1993) calculated an early Eocene (54–46 Ma) palaeopole for the Antarctic Peninsula (78°S, 21°E; α_{95} = 7.5°), on the grounds of her results and those by Dalziel *et al.* (1973) and Watts *et al.* (1986). We may calculate a late Eocene (42–38 Ma) palaeopole for East Antarctica (66°S, 322°E; α_{95} = 16.6°) by taking into account only the VGPs from the oldest of the Meander Intrusives (the Mount Monteagle and Mount McGee stocks). Comparison between the two poles (Fig. 6) can only be tentative, because their ages are different and the different locations may partly reflect the apparent polar wander from early to late Eocene. However, it is worth noting that the tilting we postulated above shifts the late Eocene palaeopole for the Meander Intrusives closer to the Antarctic Peninsula palaeopole (Fig. 6). To test this possibility, we compared the late Eocene VGPs not corrected and those corrected for a 5° rotation about the N45°E axis with the poles used by Grunow (1993) to calculate the Antarctic Peninsula palaeopole. The null hypothesis of a common mean direction fails the McFadden & Lowes (1981) test at the 95% significance level, when the Antarctic Peninsula and the uncorrected VGPs of the Meander Intrusives are tested, but passes when the tilt-corrected VGPs are considered. These results show that no final conclusions about post-Eocene relative movements between the Antarctic Peninsula and East Antarctica can be drawn until new evidence allows the possibility of a block tilting of the Meander Intrusives stocks to be ruled out altogether or more precisely defined.

Conclusions

This palaeomagnetic study of the Meander Intrusives from northern Victoria Land has resulted in determination of the first middle Tertiary (42–22 Ma) palaeomagnetic pole for East Antarctica. Its location in the Weddell Sea off the Kronprinsesse Martha Coast (69°S, 334°E; α_{95} = 9.9°) strongly supports an early Tertiary reversal of the East Antarctica APW path, as shown in the synthetic path of DiVenere *et al.* (1994).

The palaeopole has been derived from intrusive rocks which lack field evidence for or against post-emplacement tectonic movements. A regional north-westerly tilting of northern Victoria Land has been proposed as a consequence of the uplift of the Transantarctic Mountains (Roland & Tessensohn 1987, Stern & ten Brink 1989). A tilt-correction of the Meander Intrusives ChRM directions calculated according this hypothesis would move the new palaeopole closer to the synthetic APW path. Tentative comparison between the early Eocene pole for the Antarctic Peninsula (Grunow 1993) and the late Eocene pole calculated from the oldest of the Meander Intrusives stocks has shown that they differ at the 95% significance level, whereas they are no longer distinguishable if the Meander Intrusives results are corrected for a 5° north-westerly tilt. These results show that the structural geology of the coastal region of northern Victoria Land must be more clearly defined before the new Tertiary palaeomagnetic data can be used for geodynamic interpretations.

Acknowledgements

This work was supported by the Italian National Antarctic Research Programme (PNRA). RL gratefully acknowledges the logistic support of his field operations provided by ENEA at the Terra Nova Bay station. We are greatly indebted to S. Tonarini for Rb-Sr age determinations, to A. Grunow, V. DiVenere and L. Thistlewood for reviewing the manuscript and many helpful comments.

References

Armienti, P., Ghezzo, C., Innocenti, F., Manetti, P., Rocchi, S. & Tonarini, S. 1990. Palaeozoic and Cainozoic intrusives of Wilson Terrane: geochemical and isotopic data. *Memorie della Società Geologica Italiana*, **43**, 67–76.

Besse, J. & Courtillot, V. 1988. Paleogeographic maps of the continents bordering the Indian Ocean since the early Jurassic. *Journal of Geophysical Research*, **93**, 11791–11808.

BLUNDELL, D.J. 1962. Palaeomagnetic investigations in the Falkland Islands Dependencies. *British Antarctic Survey Scientific Reports*, No. 39, 24 pp.

BOSUM, W., DAMASKE, D., ROLAND, N.W., BEHRENDT, J. & SALTUS, R. 1989. The GANOVEX IV Victoria Land/Ross Sea aeromagnetic survey: interpretation of the anomalies. *Geologisches Jahrbuch*, **E 38**, 153–230.

CANDE, S.C. & KENT, D.V. 1992. A new geomagnetic polarity time scale for the late Cretaceous and Cenozoic. *Journal of Geophysical Research*, **97**, 13917–13951.

CARMICHAEL, C.M. 1967. The iron-titanium oxides of salic volcanic rocks and their associated ferromagnesian silicates. *Contributions to Mineralogy and Petrology*, **14**, 36–64.

DALZIEL, I.W.D., LOWRIE, W., KLIGFIELD, R. & OPDYKE, N.D. 1973. Paleomagnetic data from the southernmost Andes and the Antarctandes. *In* TARLING, D.H. & RUNCORN, S.K., *eds. Implication of continental drift to the Earth Sciences*. New York: Academic Press, 87–101.

DEER, W.A., HOWIE, R.A. & ZUSSMAN, J. 1992. *An introduction to the rock-forming minerals*. Harlow: Longman, 695 pp.

DIVENERE, V.J., KENT, D.V. & DALZIEL, I.W.D. 1994. Mid-Cretaceous paleomagnetic results from Marie Byrd Land, West Antarctica: A test for post-100 Ma relative motion between East and West Antarctica. *Journal of Geophysical Research*, **99**, 15115–15139.

DUNCUMB, P. & REED, S.J.B. 1968. The calculation of stopping power and backscatter effect in electron probe microanalysis. *In* HEINRICH, K.F.J., *ed. Quantitative electron probe microanalysis*. Washington DC: National Bureau of Standards, Special Publication No. 298, 133–154.

EMBLETON, B.J.J. & MCELHINNY, M.W. 1982. Marine magnetic anomalies, palaeomagnetism and the drift history of Gondwanaland. *Earth and Planetary Science Letters*, **58**, 141–150.

EWART, A., OVERSBY, V.M. & MATEEN, A. 1977. Petrology and isotope geochemistry of Tertiary lavas from the northern flank of the Tweed Volcano, southeastern Queensland. *Journal of Petrology*, **18**, 73–113.

FITZGERALD, P.G. & GLEADOW, A.J.W. 1988. Fission-track geochronology, tectonics and structure of the Transantarctic Mountains in northern Victoria Land, Antarctica. *Chemical Geology (Isotope Geoscience Section)*, **73**, 169–198.

GANOVEX Team. 1987. Geological map of North Victoria Land, Antarctica, 1: 500 000, Explanatory Notes. *Geologisches Jahrbuch*, **B 66**, 7–80.

GRUNOW, A.M. 1993. New paleomagnetic data from the Antarctic Peninsula and their tectonic implications. *Journal of Geophysical Research*, **98**, 13815–13833.

HAGGERTY, S.E. 1976a. Oxidation of opaque mineral oxides in basalts. *In* RUMBLE, D., *ed. Oxide minerals*. Mineralogical Society of America, Reviews in Mineralogy, No. 3, Hg1-Hg98.

HAGGERTY, S.E. 1976b. Opaque mineral oxides in terrestrial igneous rocks. *In* RUMBLE, D., *ed. Oxide minerals*. Mineralogical Society of America, Reviews in Mineralogy, No. 3, Hg101-Hg277.

HAGGERTY, S.E. 1991. Oxide textures — A mini-atlas. *In* LINDSLEY, D.H., *ed. Oxide minerals: petrology and magnetic significance*. Mineralogical Society of America, Reviews in Mineralogy, No. 25, 129–219.

KRETZ, R. 1983. Symbols for rock-forming minerals. *American Mineralogist*, **68**, 277–279.

LANZA, R. & ZANELLA, E. 1993. Palaeomagnetism of the Ferrar dolerite in the northern Prince Albert Mountains (Victoria Land, Antarctica). *Geophysical Journal International*, **114**, 501–511.

LAWVER, L.A., SCLATER, J.G. & MEINKE, L. 1985. Mesozoic and Cenozoic reconstructions of the south Atlantic. *Tectonophysics*, **114**, 233–254.

LIVERMORE, R.A. & WOOLLET, R.W. 1993. Sea-floor spreading in the Weddell Sea and southwest Atlantic since late Cretaceous. *Earth and Planetary Science Letters*, **117**, 475–495.

LOCK, J. & MCELHINNY, M.W. 1991. The global paleomagnetic database. *Surveys in Geophysics*, **12**, 317–491.

MCFADDEN, P.L. & LOWES, F.J. 1981. The discrimination of mean directions drawn from Fisher distributions. *Geophysical Journal of the Royal Astronomical Society*, **67**, 19–33.

MANKINEN, E.A. & COX, A. 1988. Paleomagnetic investigation of some volcanic rocks from the McMurdo volcanic province, Antarctica. *Journal of Geophysical Research*, **93**, 11599–11612.

MAYES, C.L., LAWVER, L.A. & SANDWELL, D.T. 1990. Tectonic history and new isochron chart of the South Pacific. *Journal of Geophysical Research*, **95**, 8543–8567.

MÜLLER, P., SCHMIDT-THOMÉ, M., KREUZER, H., TESSENSOHN, F. & VETTER, U. 1991. Cenozoic peralkaline magmatism at the western margin of the Ross Sea, Antarctica. *Memorie della Società Geologica Italiana*, **46**, 315–336.

NATHAN, S. 1971. Geology and petrology of the Campbell-Aviator divide, Northern Victoria Land, Antarctica. Part 2 — Palaeozoic and Precambrian rocks. *New Zealand Journal of Geology and Geophysics*, **14**, 564–596.

PIPER, J.D.A. 1988. *Palaeomagnetic database*. Milton Keynes: Open University Press, 264 pp.

ROLAND, N.W. & TESSENSOHN, F. 1987. Rennick faulting - an early phase of Ross Sea rifting. *Geologisches Jahrbuch*, **B 66**, 203-230.

ROYER, J.Y., PATRIAT, P., BERGH, H. & SCOTESE, C.R. 1988. Evolution of the Southwest Indian Ridge from the Late Cretaceous (anomaly 34) to the Middle Eocene (anomaly 20). *Tectonophysics*, **155**, 235–260.

SCHNEIDER, D.A. & KENT, D.V. 1990. Testing models of the Tertiary paleomagnetic field. *Earth and Planetary Science Letters*, **101**, 260–271.

STAGG, H.M.J. & WILLCOX, J.B. 1992. A case for Australia-Antarctica separation in the Neocomian (*c.* 125 Ma). *Tectonophysics*, **210**, 21–32.

STEINTHORSSON, S., HELGASON, O., MADSEN, M.B., BENDER KOCH, C. BENTZON, M.D. & MORUP, S. 1992. Maghemite in Icelandic basalts. *Mineralogical Magazine*, **56**, 185–199.

STERN, T.A. & TEN BRINK, U.S. 1989. Flexural uplift of the Transantarctic Mountains. *Journal of Geophysical Research*, **94**, 10315–10330.

STUMP, E., HOLLOWAY, J.R., BORG, S.G. & ARMSTRONG, R.L. 1983. Discovery of a Tertiary granite pluton, northern Victoria Land. *Antarctic Journal of the United States*, **18** (5), 17–18.

STUMP, E.S. & FITZGERALD, P.G. 1992. Episodic uplift of the Transantarctic Mountains. *Geology*, **20**, 161–164.

TAUXE, L., BESSE, J. & LABRECQUE, J. 1983. Palaeolatitudes from DSDP Leg 73 sediments cores: implications for the apparent polar wander path for Africa during the late Mesozoic and Cenozoic. *Geophysical Journal of the Royal Astronomical Society*, **73**, 315–324.

ULMER, P. 1986. *NORM-Program for cation and oxygen mineral norms*. Zürich: Computer Library IKP-ETH.

VALENCIO, D.A., MENDIA, J.E. & VILAS, J.F. 1979. Palaeomagnetism and K-Ar age of Mesozoic and Cenozoic igneous rocks from Antarctica. *Earth and Planetary Science Letters*, **45**, 61–68.

VEEVERS, J.J. & EITTREIM, S.L. 1988. Reconstruction of Antarctica and Australia at breakup (95 ± 5 Ma) and before rifting (160 Ma). *Australian Journal of Earth Sciences*, **35**, 355–362.

WALKER, B.C. 1983. The Beacon Supergroup of northern Victoria Land, Antarctica. *In* OLIVER, R.L., JAMES, P.R. & JAGO, J.B., *eds. Antarctic earth sciences*. Canberra: Australian Academy of Sciences, 211–214.

WATTS, D.R., WATTS, G.C. & BRAMALL, A.M. 1984. Cretaceous and early Tertiary paleomagnetic results from the Antarctic Peninsula. *Tectonics*, **3**, 333–346.